Chapter 4

Experimental results

4.1 Raw material characterizations

4.1.1 Particle size distribution

The particle size distribution results of all compositions are shown in Fig.4.1. The average particle size of all compositions are in the range of 0.5 – 0.8 μm.

The average particle size of composition 2.1 – 2.5 are in the range of 0.55 - 0.67 μm and that of 2.6 – 2.10 are 0.65 - 0.78 μm. Therefore the average particle size of AKP-30 is a little smaller than the average particle size of AES-11, in the same tendency with the data from supplier shown in Table 3.1.

The particle size distribution of 2.2 – 2.5 and 2.7 – 2.10 are almost the same with that of 2.1 and 2.6. Therefore, Al_2O_3 particles were not ground properly by the mixing process.

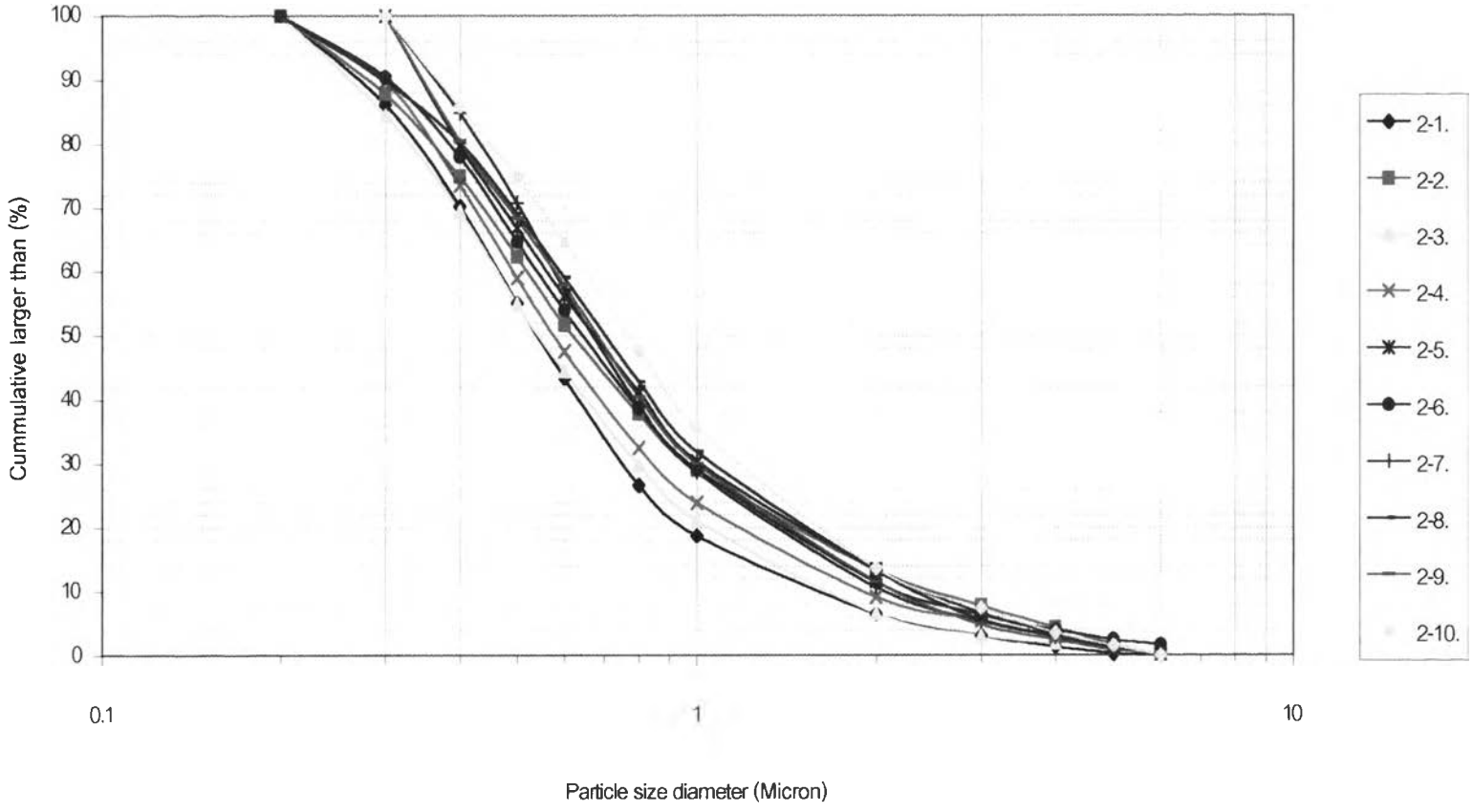

Fig.4.1 Particle size distribution of AKP-30 and AES-11 alumina powders.

4.1.2 Shape of alumina powder

SEM micrographs of pure AKP-30 and pure AES-11 alumina powders are shown in Fig.4.2 (a) and (b), respectively. AKP-30 has smaller grain size than AES-11 as shown in these figures.

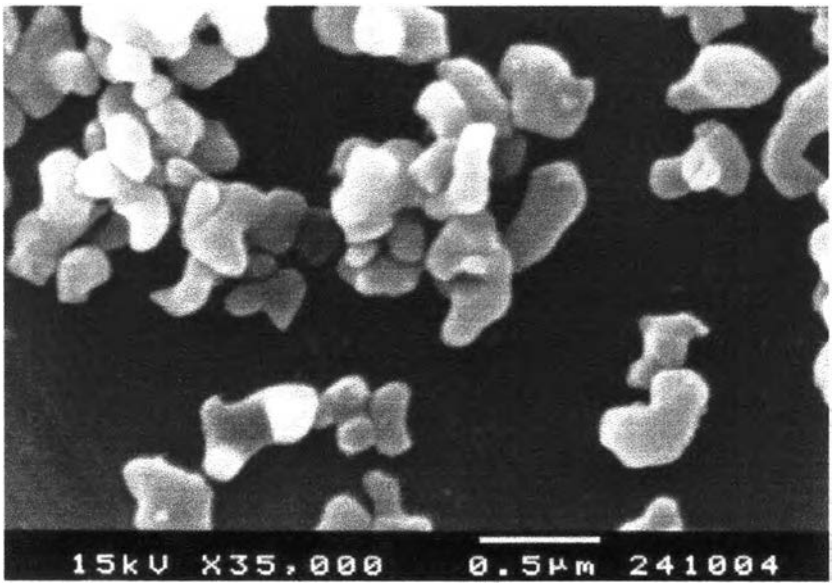

Fig.4.2(a) Microstructure of pure AKP-30 alumina powder.

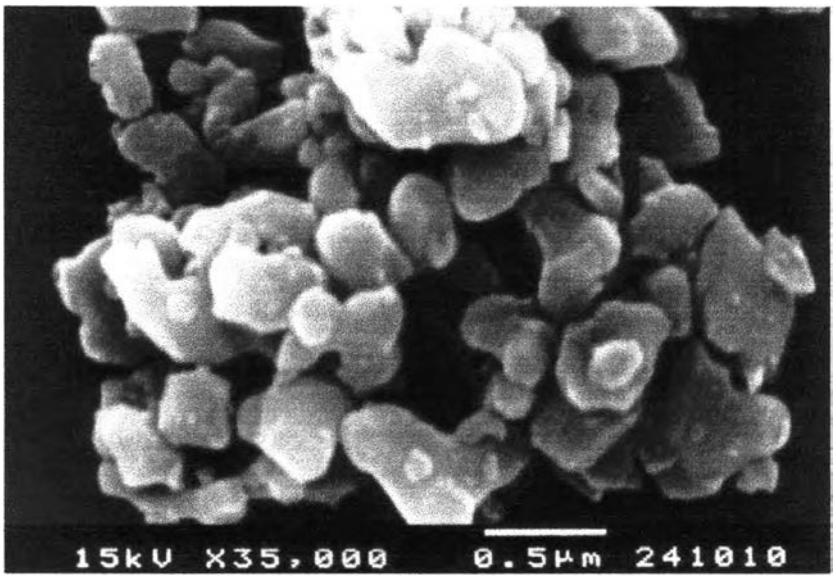

Fig.4.2(b) Microstructure of pure AES-11 alumina powder.

4.2 Preliminary sintering of AES-11 and AKP-30

Pure AES-11 and AKP-30 alumina pellets were formed with 25 mm diameter and sintered at 1450-1650 ^{o}C for 2 hrs. Specific gravity, water absorption and relative density were measured as shown in Appendix 4. Relationship between relative density and sintering temperature of all specimens are shown in Appendix 5. The relationship between relative density and sintering temperature is shown in Fig.4.3(a) and (b), AKP-30 and AES-11, respectively. The dependence of density on sintering temperature is observed. Relative density increases with sintering temperature. Density reached to almost full at 1600-1650 ^{o}C whereby the density at 1600 and 1650 ^{o}C are almost same in case of AKP-30. AKP-30 is easier to sinter to full density at 1550-1650 ^{o}C than AES-11 because of AKP-30 its smaller grain size as shown in Fig.4.2.

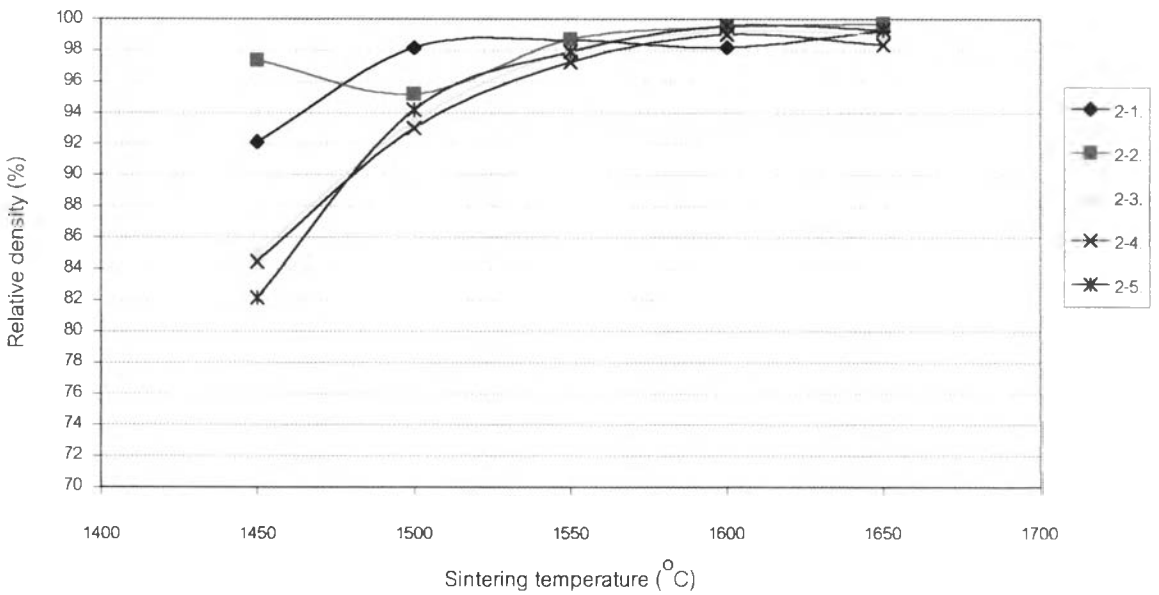

Fig.4.3(a)The relationship between relative density and sintering temperature of AKP-30.

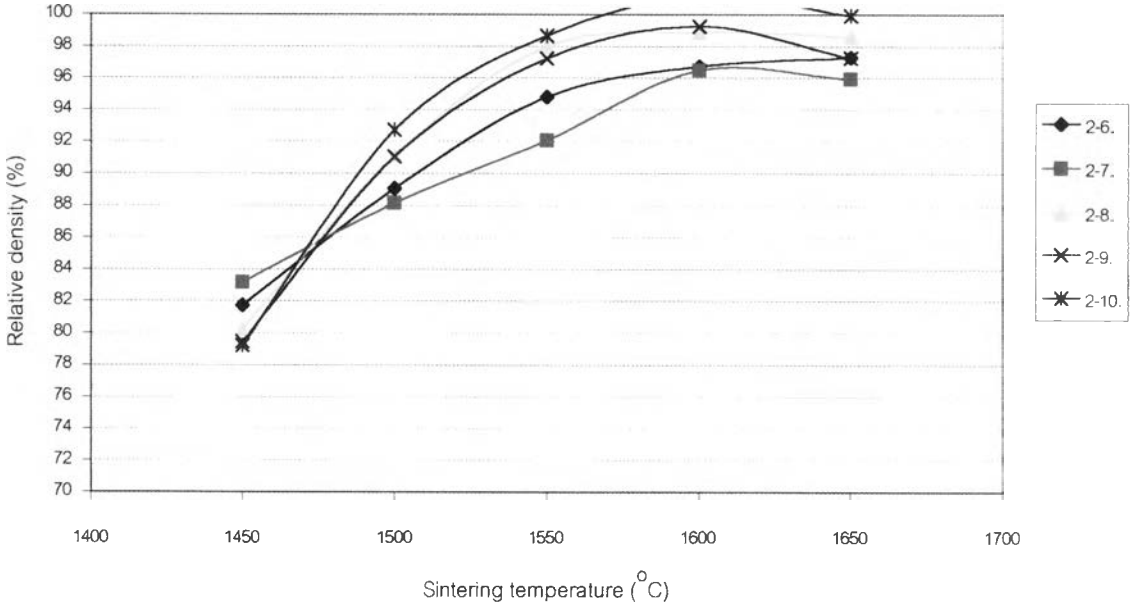

Fig.4.3(b)The relationship between relative density and sintering temperature of AES-11.

4.3 Thermal conductivity and microstructure of AES-11 and AKP-30

In section 4.2, AES-11 and AKP-30 can be sintered to almost full density at 1600-1650 ^{o}C. Then, specimens for measuring thermal conductivity and for SEM observation are sintered at 1650 ^{o}C. In this experiment, 12 mm diameter die was used because the diameter of specimen which will be measured thermal conductivity should be in the range of 9.5-10.5 mm diameter. Three to five pieces of specimens for each composition were sintered. The results of specific gravity, water absorption, relative density of this set of specimens are shown in Appendix 6.

Thermal conductivity of each of composition 2.1 – 2.10 are shown in Table 4.1. Thermal conductivities of AKP-30 are higher than 30 W/m·K for all compositions of MgO doped AKP-30 showed the highest thermal conductivity.

Table 4.1 Thermal conductivity of doped and pure AKP-30 and AES-11 alumina specimens sintered at 1650 ^{o}C for 2 h.

composition			Specific gravity	Relative density (%)	Thermal conductivity (W/m·K)
AKP-30	Undoped		3.84	96.7	35.5
	MgO 0.5%		3.91	98.5	37.2
	ZrO_2	1.5%	3.78	94.7	34.1
		3.0%	3.88	96.7	30.8
		7.5%	3.92	96.2	30.1
AES-11	Undoped		3.83	96.5	31.8
	MgO 0.5%		3.82	96.3	30.8
	ZrO_2	1.5%	3.91	98.0	31.4
		3.0%	3.92	97.7	33.5
		7.5%	3.99	97.9	29.8

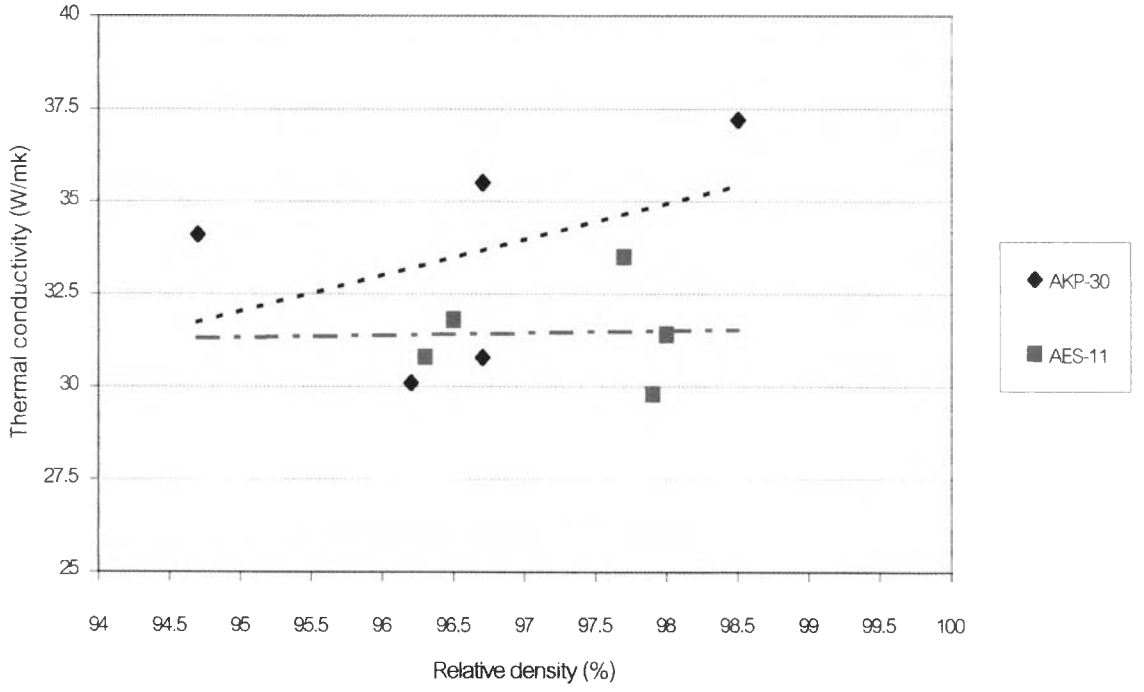

Fig.4.4 Relationship between relative density and thermal conductivity of AKP-30 and AES-11.

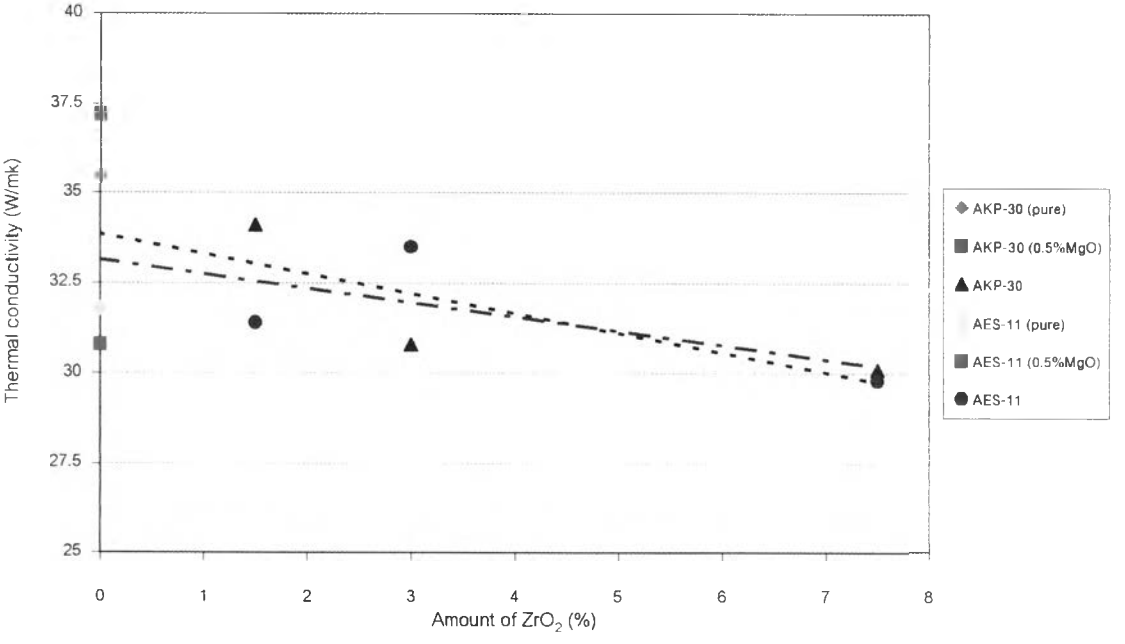

Fig.4.5 Relationship between the amount of ZrO_2 and thermal conductivity of AKP-30 and AES-11.

Fig.4.4 shows the relationship between the relative density and the thermal conductivity. There is a slight tendency that a specimen of higher relative density shows higher thermal conductivity. However, the relationship is not desirable.

Fig.4.5 shows the relationship between the amount of ZrO_2 and the thermal conductivity. There is also a tendency that specimens containing high concentration of ZrO_2 show slightly lower thermal conductivity. But the deviation of the data is significant and the reliability of the tendency is not desirable.

The effects of relative density and ZrO_2 content on thermal conductivity will be discussed in section 5.5.

SEM photographs are attached to Appendix 7. As shown in Fig 4.6 (a) and (b), AKP-30 has narrow grain size distribution and equiaxial grain shape while AES-11 has available wide grain size distribution and equiaxial grain shape. Table 4.2 and Fig.4.7 shows the relationship between the amount of ZrO_2 and the average grain size of AKP-30 and AES-11. As shown in the figure, the grain sizes of AKP-30 are a little larger than that of AES-11. The average grain size decreased with an increase of the ZrO_2 content. Most of ZrO_2 particles are at the grain boundaries, particular at the triple points, and the size of ZrO_2 particles are smaller than that of Al_2O_3, as shown in Fig.4.6 (a) and (b).

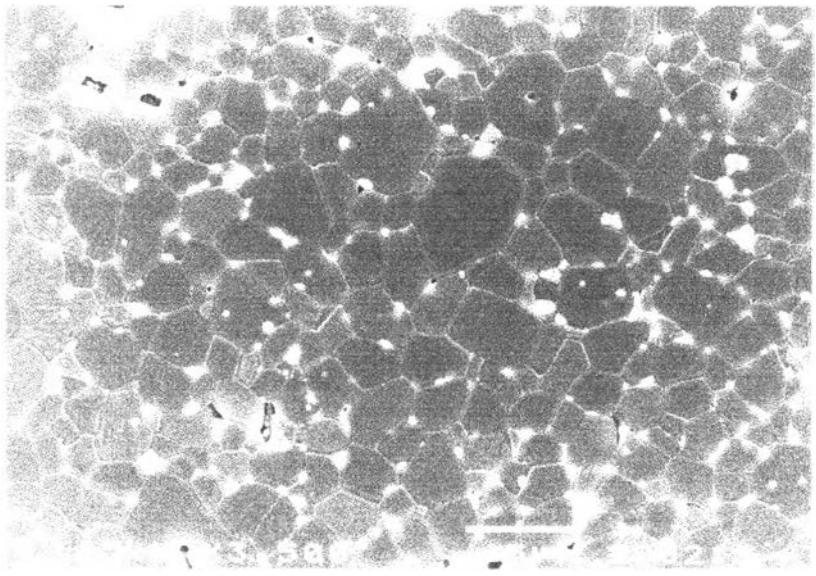

Fig.4.6(a) SEM photograph of 7.5% ZrO_2 doped AKP-30.

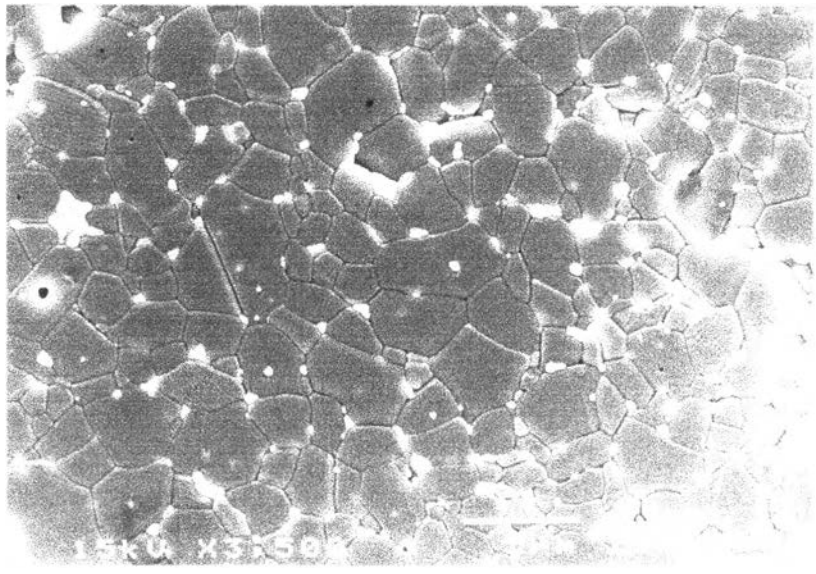

Fig.4.6(b) SEM photograph of 7.5%ZrO_2 doped AES-11.

Table 4.2 The average grain size of alumina sintered at 1650 ^{O}C for 2 h.

Composition			Average grain size (micron)
AKP-30	Undoped		3.58
	MgO 0.5%		3.41
	ZrO_2	1.5%	2.82
		3.0%	3.96
		7.5%	1.66
AES-11	Undoped		2.04
	MgO 0.5%		1.94
	ZrO_2	1.5%	2.12
		3.0%	1.91
		7.5%	1.76

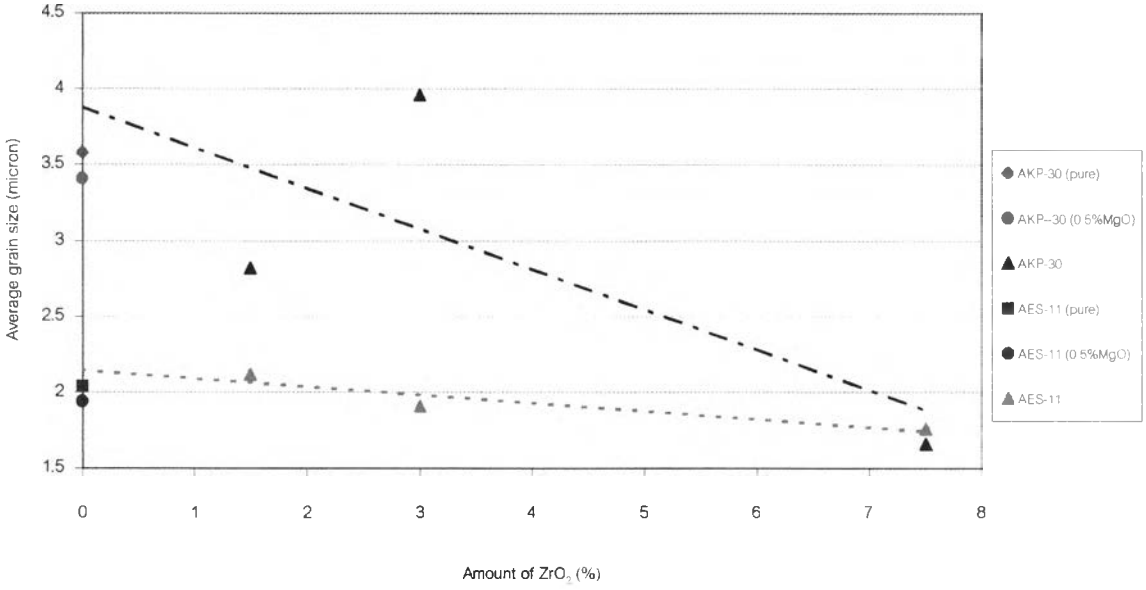

Fig.4.7 Relationship between the amount of ZrO_2 and the average grain size of AKP-30 and AES-11.

4.4 Mechanical properties of AES-11

In this experiment, the average grain size of AES-11 is smaller than AKP-30 for most of compositions shown in Table4.2. It is expected that the mechanical strength of AES-11 is higher than AKP-30. So that, in this experiment, only AES-11 was used for mechanical strength measurement.

Specific gravity, water absorption, thickness, radius of specimens, mechanical strength, fractures of specimens, and surface roughness are shown in appendix 8, 9, 10, 11 and 12, respectively. Thickness and radius of each specimen were used to calculate mechanical strength using equation (3.5). The relationship between mechanical strength and sintering temperature are shown in Fig.4.8. As shown in Appendix 8 and Fig.4.9 and 4.10 specimens sintered at 1450 and 1500 ^{O}C were low in relative density and high in porosity. Presence of the pores is thought to be the cause of lower strength. As shown in Appendix 12, average surface roughness (Ra) is as small as 0.11, 0.09, 0.24, 0.18 and 0.30 μm for sintering temperature of 1450, 1500, 1550, 1600 and 1650 ^{O}C, respectively. However, there are a few rather sharp holes about 3-5, 2, 3-4, 1.5 and 3-6 μm, respectively. Since ceramics usually breaks due to presence of pores, an inclusion and surface cracks fracture surface were observed to detect fracture origin using an optical microscope. However, we could not find the obvious fracture origin due to the white colour of specimens. As shown in Fig.4.8, mechanical strength of the specimen sintered at 1600 ^{O}C was highest in average. Most of specimens sintered at 1550, 1600 and 1650 ^{O}C attained over the target value, 400 MPa.

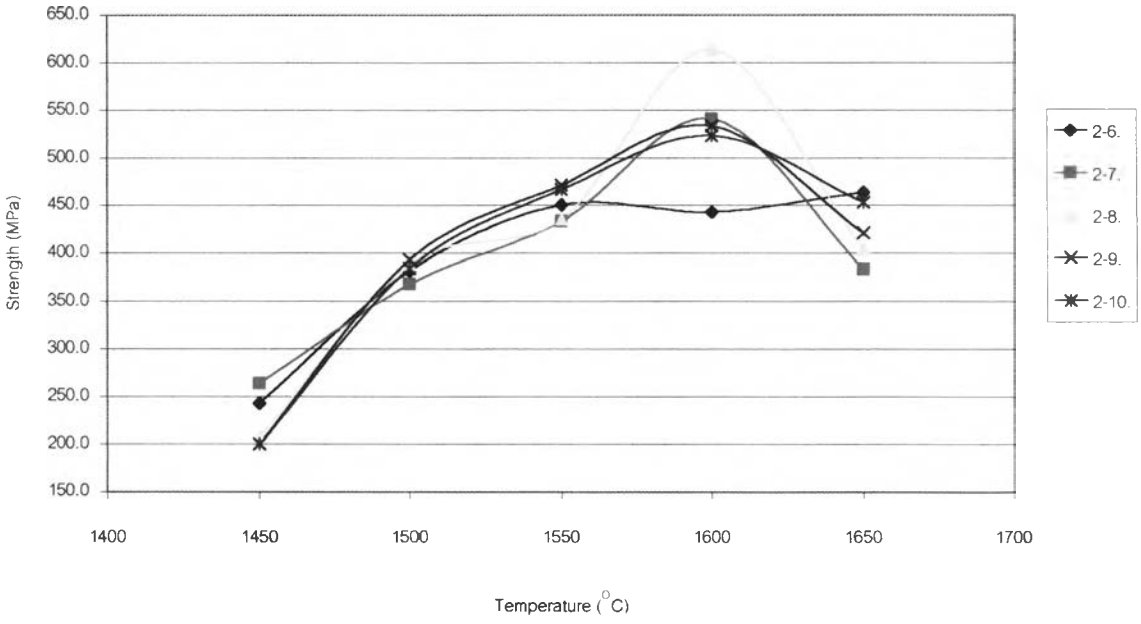

Fig.4.8 The relationship between strength and sintering temperature of AES-11.

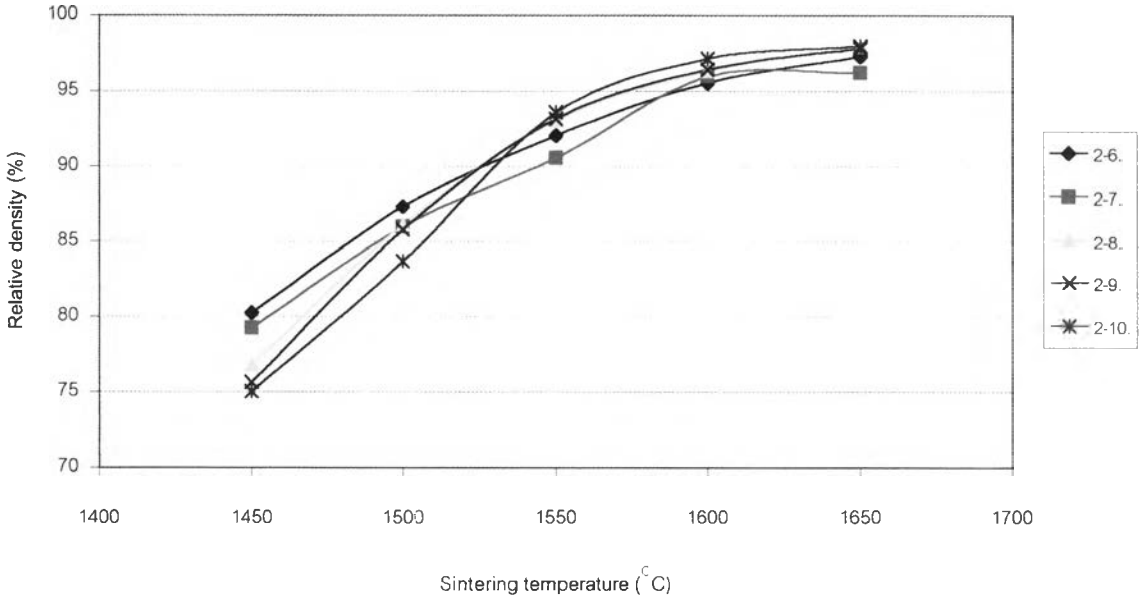

Fig.4.9 The relationship between relative density and sintering temperature of AES-11.

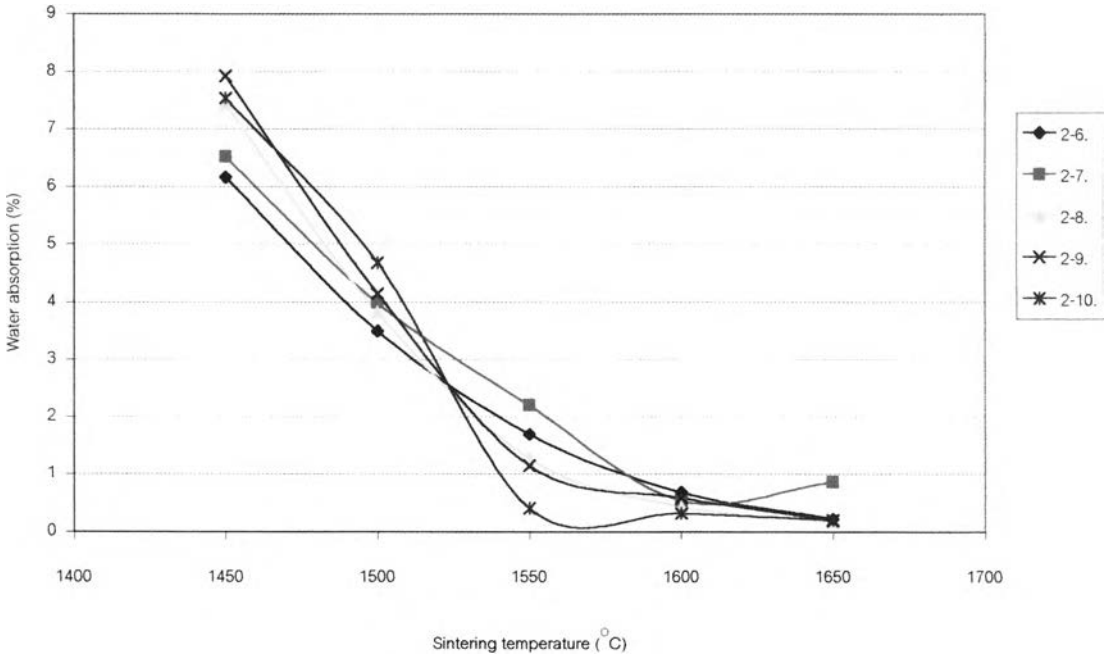

Fig.4.10 The relationship between water absorption and sintering temperature of AES-11.

4.5 The effect of sintering time of AES-11

In section 4.2, the study of the effect of sintering time, all specimens were sintered at 1450 – 1650 ^{O}C for 2 hrs fired soaking time. In this section, the soaking times were varied from 1, 4, and 6 hrs to study the effects of sintering time. All data are shown in Appendix 13 and 14. The relations between sintering time, relative density and sintering temperature of each composition of AES-11 are shown in Appendix 14 (a) - (e). The data for 2 hrs are referred from previous section and shown in Appendix 4.

When the sintering temperatures are as low as 1450 and 1500 ^{O}C, density gradually increased with soaking time. On the otherhand, density at 1 soaking hour is almost same as that of 2-6 soaking hours when sintering temperature is over 1550 ^{O}C, as shown in Fig.4.11.

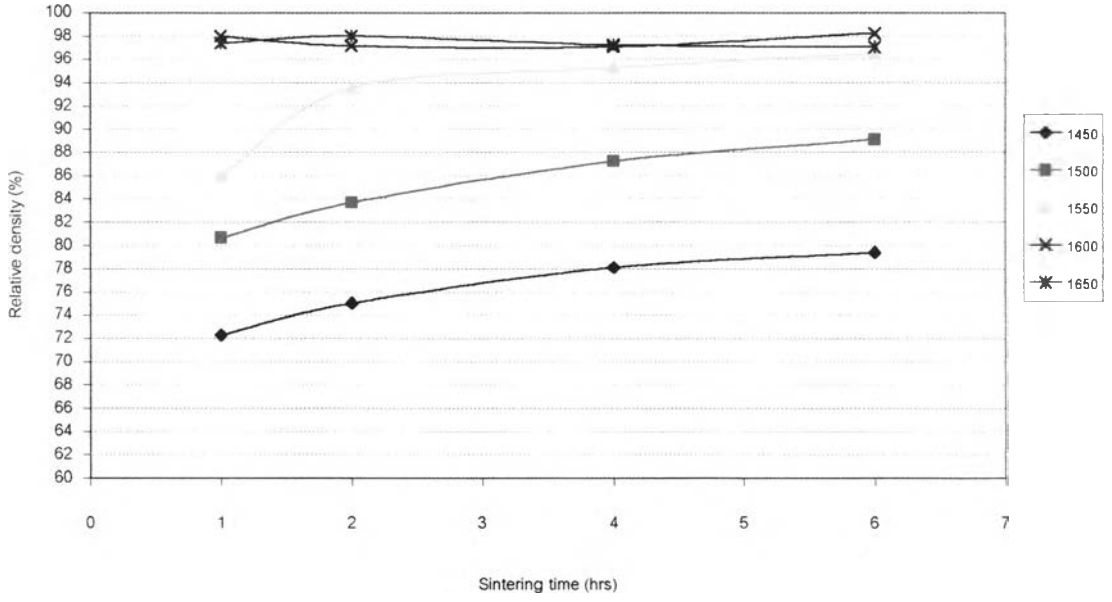

Fig.4.11 The relationship between sintering time, relative density and sintering temperature of AES-11 doped with 7.5% ZrO_2.

As shown in 5.4, grain size of specimens sintered at 1650 ^{o}C for 2 hrs were larger than that sintered at 1600 ^{o}C for 2 hrs. In this experiment were not observed the grain size of specimens sintered at 4 and 6 hrs. However, the grain growth is supposed to grow with longer soaking time. Generally, grain growth reduces the mechanical strength. Then, two hours soaking time will be reasonable for the standpoint of mechanical strength.

4.6 Sintering of mixed additives at 1450 – 1650 ^{o}C

As shown in 4.3, ZrO_2 particles were observed mostly at the grain boundaries. Specimens with MgO showed beautiful grain shape. In this section, the effects of mixed additive were studied by adding both MgO and ZrO_2 in the same composition. To check the reproducibility of the results, specimens were sintered twice at each temperature and each specimen was measured twice. Specific gravity, water absorption and relative density were measured as shown in Appendix 15 and 16. As seen in Appendix 16, the relative density of specimen No.1 sintered at 1450 ^{o}C were higher than 84%. On the other hand, that of specimen No.2 and data seen in Fig.4.3 (a) and (b) are less than 78% and 85%, respectively. There was a significant differences in the relative density measurement. Unfortunately the cause of the difference was not determine.

Comparing the data of Fig.4.3 (a),(2-3, 2-4, 2-5) and (b),(2-8, 2-9, 2-10) with Appendix 16 (c) and (d), these are 3 – 4% difference in the relative density values at each sintering temperature. However, the tendencies of the relative density vs. sintering temperature were similar.

Microstructure, thermal conductivity and mechanical property of these mixed additive compositions were not measured due to the limitation of time. The conclusions of the effects of mixed additive could not be drawn due to the insufficient data.